Biochemical Pharmacology, Vol. 59, pp. 1501–1511, 2000.

ISSN 0006-2952/00/$–see front matter
PII S0006-2952(00)00281-1

Regional and Cellular Induction of Nicotine-Metabolizing CYP2B1 in Rat Brain by Chronic Nicotine Treatment

*Sharon Miksys, Ewa Hoffmann and Rachel F. Tyndale**

Centre for Addiction and Mental Health and Department of Pharmacology, University of Toronto, Toronto, Ontario, Canada M5S 1A8

ABSTRACT. In the rat, nicotine is metabolized to cotinine primarily by hepatic cytochrome P450 (CYP) 2B1. This enzyme is also found in other organs such as the lung and the brain. Hepatic nicotine metabolism is unaltered after nicotine exposure; however, nicotine may regulate CYP2B1 in other tissues. We hypothesized that nicotine induces its own metabolism in brain by increasing CYP2B1. Male rats were treated with nicotine (0.0, 0.1, 0.3, or 1.0 mg base/kg in saline) s.c. daily for 7 days. CYP2B1 mRNA and protein were assayed in the brain and liver by reverse transcriptase-polymerase chain reaction (RT-PCR), immunoblotting, and immunocytochemistry. In control rats, CYP2B1 mRNA and protein expression were brain region- and cell-specific. CYP2B1 was not induced in the liver, but CYP2B1 mRNA and protein showed dose-dependent, region- and cell-specific patterns of induction across brain regions. At 1.0 mg nicotine/kg, the largest increase in protein was in the brain stem (5.8-fold, $P < 0.05$) with a corresponding increase in CYP2B1 mRNA (7.6-fold, $P < 0.05$). Induction of CYP2B1 was also observed in the frontal cortex, striatum, and olfactory tubercle. Immunocytochemistry showed that induction was restricted principally to neurons. These data indicate that nicotine may alter its own metabolism in the brain through transcriptional regulation, perhaps contributing to central tolerance to the effects of nicotine. CYP2B1 and its human homologue CYP2B6 also activate tobacco smoke procarcinogens such as NNK [4-(methylnitrosamino)-1-(3-pyridyl)-1-butanone]. Highly localized increases in CYP2B could result in increased mutagenesis. These data suggest roles for nicotine-induced CYP2B in central metabolic tolerance, nicotine-induced neurotoxicity, neuroplasticity, and carcinogenesis. BIOCHEM PHARMACOL **59**;12:1501–1511, 2000. © 2000 Elsevier Science Inc.

KEY WORDS. brain; CYP2B; cytochrome P450; drug metabolism; neurotoxicity; nicotine

CYPs† have been identified as functional enzymes in the central nervous system, where they are inducible, and are known to metabolize a number of exogenous and endogenous compounds [1]. Although the overall CYP content of the rat brain is lower than that of the liver, individual CYPs have been identified and found to be concentrated in specific brain regions and cell types [2–6]. This indicates that in certain areas of the brain they may reach levels similar to those found in the liver. This restricted expression suggests that in discrete brain cells or regions there may be significant levels of metabolism resulting in altered local drug and metabolite concentrations unlikely to be detected in the plasma. This highly localized metabolism may also contribute to specific cellular damage resulting from toxic CYP metabolites.

The CYP2B family metabolizes a number of drugs, xenobiotics, and steroids, including nicotine, NNK, aromatic hydrocarbons, and the anticancer prodrug cyclophosphamide [7, 8]. Both CYP2B1 and CYP2B2 enzymes have been identified in rat brain and neural tissue; however, CYP2B2 mRNA is expressed at very low levels [9, 10]. Like their hepatic forms, these isozymes are inducible by phenobarbital, but with complex patterns specific to brain region and cell type [10, 11].

Nicotine is the major constituent of tobacco that is responsible for tobacco dependence. It is absorbed through the lung epithelium and travels directly to the brain, bypassing the liver, where it readily crosses the blood–brain barrier. In humans, more than 70% of nicotine is inactivated to cotinine by hepatic CYP2A6 via the formation of the $\Delta^{1'(5')}$-iminium ion [12, 13]. In rats, hepatic CYP2A enzymes do not metabolize nicotine; rather, CYP2B1 is the primary CYP responsible for the conversion of nicotine to cotinine by a similar pathway [14, 15], although to a lesser degree [16]. Human CYP2B6 can also metabolize nicotine; however, it is found at low levels in human liver and makes only a minor contribution to human hepatic nicotine metabolism [12]. In addition to rat liver, rat brain is also

* Corresponding author: Dr. Rachel F. Tyndale, Department of Pharmacology, 1 Kingís College Circle, University of Toronto, Toronto, Canada M5S 1A8. Tel. (416) 978-6374; FAX (416) 978-6395; E-mail: r.tyndale@utoronto.ca

† *Abbreviations*: BROD, benzyloxyresorufin *O*-dealkylase; CYP, cytochrome P450; NDMA, *N*-nitrosodimethylamine; NNK, 4-(methylnitrosamino)-1-(3-pyridyl)-1-butanone; PROD, pentoxyresorufin *O*-dealkylase; and RT–PCR, reverse transcriptase–polymerase chain reaction.

Received 2 June 1999; accepted 8 November 1999.

able to convert nicotine to cotinine [17]. Multiple metabolites including cotinine are found in rat brain after peripheral administration of nicotine [18], and although it is unclear whether they are formed by brain or peripheral metabolism, cotinine has been shown to be pharmacologically active in rat brain [19].

It is well-established that nicotine exerts its neuropharmacological effects by acting on nicotinic acetylcholine receptors in the brain, and that these receptors are up-regulated in response to chronic nicotine administration in animal models [20] and in human smokers [21]. Animals and humans develop tolerance to the pharmacological effects of nicotine, and this involves, but cannot be explained fully by, desensitization of nicotinic cholinergic receptors [22, 23]. Anandatheerthavarada *et al.* [24] found that chronic nicotine increased PROD and BROD activity in some rat brain regions, suggesting CYP2B1 induction. These data together indicate that there may be a role for brain nicotine metabolism by CYP2B1 in the development of tolerance to nicotine, i.e. central metabolic tolerance.

In this study, we used a combination of immunoblotting, immunohistochemistry, and RT–PCR to determine the extent of induction of CYP2B1 by nicotine in the brain and liver, and the molecular level at which this induction occurs. In addition, we investigated the dose-dependency as well as the region- and cell-specificity of nicotine induction of CYP2B1.

MATERIALS AND METHODS

Animals

Four groups (N = 6 per group) of adult male Wistar rats (250–300 g; Charles River) were injected s.c., once per day, for 7 days with 0, 0.1, 0.3, or 1.0 mg nicotine base/kg body weight, in the form of nicotine bitartrate (Sigma) in sterile saline adjusted to pH 7.4. The doses used in this study provided a range that was both behaviorally and pharmacologically relevant. This range included doses at which rats develop nicotine tolerance (0.4 mg/kg over 12 days, continuous infusion, e.g. Ref. 25), which rats will self-administer (to a maximum of 0.5 mg nicotine base/kg over 1 hr, e.g. Ref. 26), which up-regulate nicotinic acetylcholine receptors in rat brain (0.45 to 2.0 mg/kg, e.g. Refs. 27 and 28), and which increase CYP2B1-mediated PROD activity (1.2 mg nicotine base/kg/day s.c., Ref. 24). Four hours after the last injection, animals were decapitated, and brains and livers were removed. Four hours is the approximate half-life of phenobarbital-induced hepatic CYP2B1 mRNA, and is less than the 16- to 20-hr half-life reported for phenobarbital-induced hepatic CY2B1 apoprotein [29]. Livers were frozen in liquid nitrogen and stored at −80° until used for membrane preparation or total RNA extraction. Brains were divided longitudinally into 12 halves per dose (N = 6 rats per dose). For each dose, four halves from different animals were processed for each of three assays: four halves for immunocytochemistry, four halves for membrane preparation for immunoblotting, and four halves for RNA extraction. For immunoblotting and RT-PCR, half brains were dissected into seven regions, frozen immediately in liquid nitrogen, and stored at −80°. These regions were chosen to include those used by Anandatheerthavarada *et al.* [24] and to include regions known to express nicotinic acetylcholine receptors, which are regulated by nicotine. Whole brains from an additional six untreated male Wistar rats were dissected into twelve regions, which were pooled for membrane preparation for immunoblotting. All dissections were performed according to the Paxinos and Watson [30] stereotaxic atlas of the rat brain. The experimental procedures described in this study were carried out in accordance with the guidelines for the care and use of laboratory animals and approved by the Animal Care Committee of the University of Toronto.

Immunoblotting

Brain regions were homogenized manually in 100 mM Tris (pH 7.4) with 0.1 mM EDTA and 0.32 M sucrose on ice. As it has been reported that brain CYPs are present in microsomal and mitochondrial membranes [31], we prepared brain membranes containing both mitochondrial and microsomal CYPs. Briefly, homogenates were centrifuged at 3000 *g* for 5 min to remove cellular and nuclear debris, and then the supernatant was centrifuged at 110,000 *g* at 4° for 90 min to give a membrane pellet. Pellets were resuspended in 100 mM Tris (pH 7.4), 0.1 mM EDTA, 0.1 mM dithiothreitol, 1.15% (w/v) KCl, and 20% (v/v) glycerol, aliquoted into small volumes, and stored at −80°. Untreated rat liver microsomes and phenobarbital-treated rat liver microsomes (Gentest) were used as positive controls and for standard curves.

The protein content of each sample was assayed by the method of Bradford [32]. Hippocampus and liver membranes were diluted serially and used to construct standard curves. These were used to determine the linear range of detection for the immunoblotting assay. Membrane proteins (50 μg/brain region, 0.2 and 0.5 μg of induced liver microsomes as internal standard) were separated by SDS–PAGE (4% stacking and 10% separating gels), and then were transferred onto nitrocellulose membranes. Membranes were probed with a monoclonal antibody raised against rat CYP2B1 (clone number 2-66-3; a gift from Harry V. Gelboin, National Cancer Institute, NIH), which has been characterized previously [33]. CYP2B1 and CYP2B2 can be separated by molecular mass under these immunoblotting conditions; CYP2B2 migrates more slowly than the immunodetectable CYP2B1 [34]. A peroxidase-conjugated sheep anti-mouse secondary antibody was used (Roche Molecular Biochemicals) followed by enhanced chemiluminescence detection (Roche Molecular Biochemicals). Control blots were processed either without primary antibody or with primary antibody preadsorbed with 40 nM baculovirus-insect cell expressed rat CYP2B1

(Gentest). Blots were analyzed with an imaging system (Imaging Research, Inc.).

Immunocytochemistry

Half brains were fixed in 4% paraformaldehyde in 0.1 M phosphate buffer, pH 7.4, for 24 hr, cryoprotected in 20% sucrose in phosphate buffer, and rapidly frozen in isopentane cooled on dry ice. Frozen sections were collected on silane-coated slides and stored at −20° until used. Sections were washed twice in PBS (10 mM sodium phosphate buffer, 0.9% sodium chloride, pH 7.4) and incubated for 1 hr in blocking solution [PBS with 1% (w/v) skim milk powder, 2% BSA, 4% Triton X-100, and 10% normal horse serum]. Sections were incubated for 40 hr at 4° with monoclonal anti-rat CYP2B1 (clone number 4-7-1; a gift from Harry V. Gelboin), previously characterized [33], diluted 1:5000 with PBS with 2% BSA, 0.4% Triton X-100, and 2% normal horse serum. Sections were washed with PBS, incubated for 1 hr at room temperature with biotinylated horse anti-mouse IgG (Vector Laboratories Canada), and rewashed with PBS. Endogenous peroxidase activity in the sections then was quenched with 0.3% hydrogen peroxide in PBS for 5 min. The antigen-antibody complex was visualized using the avidin–biotin complex technique (ABC Elite kit, Vector Laboratories Canada) followed by reaction with 3,3′-diaminobenzidine and hydrogen peroxide (DAB kit, Vector Laboratories). Sections were dehydrated and mounted via xylene in Permount (Fisher Scientific). Control sections were incubated without primary antibody.

RT-PCR

Random hexamer primers [pd$(N)_6$], deoxynucleotide triphosphates (dNTPs), and RNA guard were obtained from Pharmacia; first strand buffer, dithiothreitol, M-MLV reverse transcriptase, and *Thermus aquaticus* polymerase were obtained from Canadian Life Technologies. RNA was extracted by a guanidinium thiocyanate single-step method [35] followed by cDNA synthesis. For each brain region, 10 μg RNA was added to first strand buffer [50 mM Tris-HCl (pH 8.4), 75 mM KCl, 3 mM $MgCl_2$, 100 mM dithiothreitol], 2.5 U pd$(N)_6$, 0.5 mM of each dNTP, 1.6 kU M-MLV reverse transcriptase, and 140 U RNA guard. cDNA synthesis was carried out in a total volume of 400 μL at 37° for 2 hr, followed by cDNA precipitation with 40 μL of 3 M sodium acetate, pH 5.2, 800 μL of 100% ethanol, and cooling to −80° for at least 30 min. PCR amplification was carried out with 3 μL cDNA template in 20 mM Tris-HCl, pH 8.4, 50 mM KCl, 4% DMSO, 0.5 mM dNTPs, 2.5 mM $MgCl_2$, 1 U *T. aquaticus* polymerase, and 0.63 mM PCR primers (forward primer 5′-GCTCAAGTACCCCCATGTCG-3′, reverse primer 5′-ATCAGTGTATGGCATTTTACTGCGG-3′) in a total volume of 20 μL. PCR was performed in a PTC thermal cycler (MJ Research, Fisher Scientific) with cycle conditions of initial denaturing at 80° for 2 min, followed by PCR amplification for 31 cycles by denaturing at 94° for 1 min, annealing at 55° for 1.5 min, and extending at 72° for 1 min.

Southern Blotting

PCR products were separated electrophoretically in 3% NuSieve (Mandel Scientific) and transferred to Zeta-Probe membranes (BioRad). Membranes were prehybridized in 50% formamide, 120 mM Na_2HPO_4, pH 7.2, 250 mM NaCl, 7% (w/v) SDS for 0.5 to 1 hr at 43°, and then hybridized in the same buffer overnight at 43° with a ^{32}P-end-labeled oligonucleotide probe specific for CYP2B1 (5′-GGTTGGTAGCCGGTGTGA-3′). The CYP2B1 PCR primers and specific oligonucleotide probe were described previously [36]. Membranes were washed with decreasing concentrations (2x, 0.5x, 0.1x) of sodium citrate saline (SSC) with 0.1% SDS for 15 min each at room temperature, and then were exposed to x-ray film at −80° for various times (18–30 hr). Autoradiograms were analyzed with an imaging system (Imaging Research Inc.).

Water blanks were used in every RT-PCR reaction to control for contaminant cDNA, RNA, or genomic DNA in PCR reactions. Primers for ubiquitous mRNA (non-neuronal enolase) were used to ensure that RNA isolation and cDNA synthesis were equally efficient for all samples [37]. Experiments were carried out at several cycles to ensure that all samples were amplified, and that their product density fell within the linear range of the standard curve of serial dilutions of liver cDNA template, which were included with every experiment. Primer pairs crossed over introns in order to identify any genomic DNA contamination, which would result in a larger size product. Genomic DNA contamination was not observed in any experiment.

Statistical Analysis

Differences between doses, brain regions, and liver were tested by ANOVA followed by the *a posteriori* Duncan's New Multiple Range Test with significance set at 5%.

RESULTS

CYP2B in Untreated Rat Brain

On immunoblots we found a single immunoreactive band in brain that comigrated with induced hepatic CYP2B1; this band was not detected when the antibody was preadsorbed with expressed rat CYP2B1 protein (inset, Fig. 1A), providing evidence that we were measuring CYP2B1 in these studies [38]. Immunoreactive protein was detected in all brain regions examined (Fig. 1). The level of CYP2B1 was much lower than that found in rat liver (approximately 80-fold less than in untreated rat liver, and 250-fold less than in phenobarbital-induced rat liver). There was some variation among brain regions (ANOVA $P = 0.02$), with a 2.5-fold difference between the region with the highest

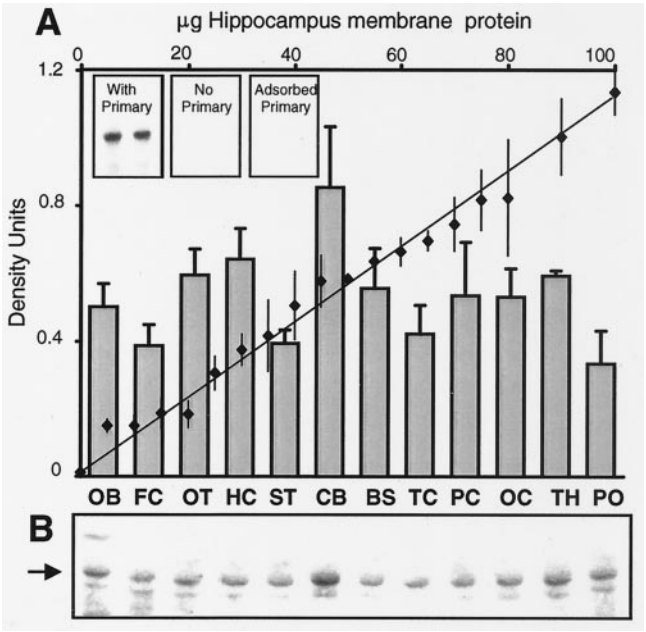

FIG. 1. (A) Distribution of CYP2B1 protein among twelve brain regions pooled from six untreated male rats. Data are means ± SEM of seven separate assays. The top x-axis of the line graph shows hippocampus membrane protein used to construct a standard curve. Data are the means ± SEM of three separate assays. Inset: Immunoblots of duplicate lanes of cerebellar membranes (50 µg protein) showed no signal in the absence of monoclonal antibody against rat CYP2B1, or in the presence of antibody adsorbed with expressed rat CYP2B1. (B) Representative immunoblot of membrane protein (50 µg) from twelve brain regions from untreated male rats. The arrow shows the position of immunoreactive CYP2B1 protein. Abbreviations: OB, olfactory bulb; FC, frontal cortex; OT, olfactory tubercle; HC, hippocampus; ST, striatum; CB, cerebellum; BS, brain stem, TC, temporal cortex; PC, parietal cortex; OC, occipital cortex; TH, thalamus; and PO, pons.

(cerebellum) and the region with the lowest (pons) amount of CYP2B1. Cerebellum was significantly higher than olfactory bulb, frontal cortex, striatum, brain stem, temporal cortex, parietal cortex, occipital cortex, and pons. Hippocampus was significantly higher than striatum and pons, and thalamus was significantly higher than pons (Fig. 1).

Induction of CYP2B by Nicotine

There was no significant change in CYP2B1 protein levels observed in the liver (Table 1). However, in the brain there was a complex pattern of region-specific increases in CYP2B1 levels with regional variation in the maximum degree of induction observed (Table 1). The largest increases were seen in the olfactory bulbs (4.3-fold) and the brain stem (5.8-fold; includes pons and medulla), with significant but modest increases in the striatum (2.1-fold), olfactory tubercle (2.1-fold; includes olfactory tubercle, piriform cortex, and anterior nucleus accumbens) and frontal cortex (1.8-fold). There were also regional differences in the lowest dose at which significant induction of CYP2B1 was observed (Table 1). Brain stem showed significant increases at all three nicotine doses (Fig. 2, Table 1). Frontal cortex showed significant increases at 0.3 mg/kg (1.6-fold) and 1.0 mg/kg (1.8-fold, Table 1). Olfactory bulbs, olfactory tubercle, and striatum showed significant increases (4.3- and 2.1-fold, respectively) only at the highest dose of nicotine, 1.0 mg/kg (Table 1). There was no significant change in cerebellum or hippocampus at any of the nicotine doses tested (Table 1). A second, very faint, higher molecular mass immunoreactive protein also appeared to be induced in brain stem (Fig. 2B), but it migrated more slowly than hepatic CYP2B2.

To ensure that the increase in CYP2B1 in the brain stem (the most highly induced region) was being measured accurately, samples were diluted to saline levels and reassayed. After appropriate dilution, CYP2B1 protein levels should have been the same for all four doses. However, they remained modestly higher for all three nicotine doses than for saline treatment (1.35-, 1.34- and 1.47-fold, respectively) indicating an underestimation of CYP2B1 in the initial analysis, and the data were adjusted accordingly.

TABLE 1. CYP2B1 protein in brain regions and liver after nicotine treatment

	Optical density (O.D.)			
		Nicotine		
Brain region	Saline	0.1 mg/kg	0.3 mg/kg	1.0 mg/kg
Olfactory bulb	0.45 ± 0.08*†	0.66 ± 0.08†	0.56 ± 0.01†	1.97 ± 0.26†‡§
Frontal cortex	0.49 ± 0.03*†	0.52 ± 0.11†	0.76 ± 0.08ddd†§	0.86 ± 0.05†§
Olfactory tubercle	0.58 ± 0.04*	0.79 ± 0.06†	0.74 ± 0.04†	1.23 ± 0.14†§
Hippocampus	0.95 ± 0.07	0.79 ± 0.13†	0.84 ± 0.07†	1.11 ± 0.17†
Striatum	0.55 ± 0.19*†	0.68 ± 0.17†	0.58 ± 0.16†	1.12 ± 0.16†§
Cerebellum	0.73 ± 0.15	0.65 ± 0.15†	0.69 ± 0.14†	0.65 ± 0.10†
Brain stem	0.88 ± 0.21	3.19 ± 0.39§	2.50 ± 0.34§	5.15 ± 0.62§
Liver	0.55 ± 0.18	0.46 ± 0.09	0.48 ± 0.10	0.52 ± 0.04

Shown are the means ± SEM of the O.D. values of CYP2B1 immunoreactive protein bands from brain membranes of four rats/dose.
*–†Significantly ($P < 0.05$) different from: *hippocampus, †brain stem, and ‡cerebellum.
§Significantly ($P < 0.05$) different from saline (between doses within the brain region).

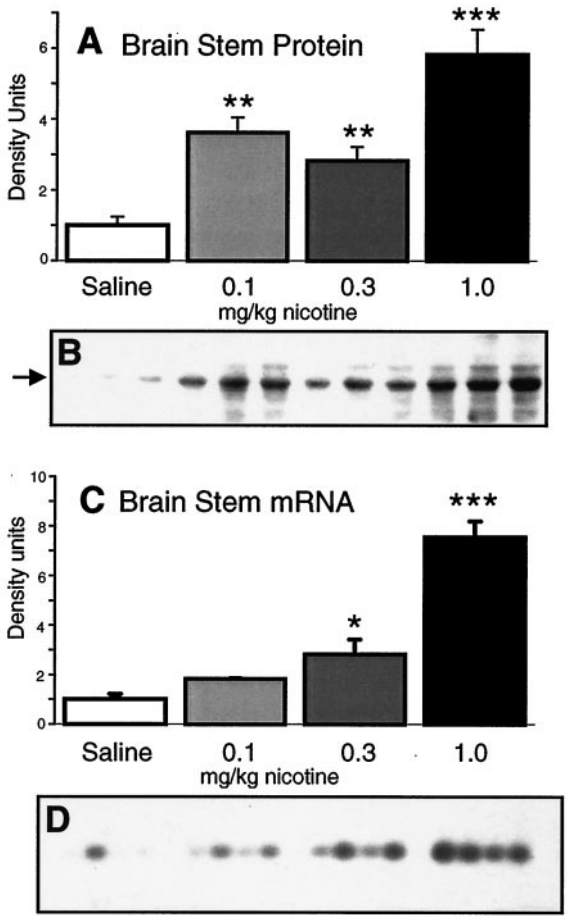

FIG. 2. Nicotine dose-dependent increase in CYP2B1 protein and mRNA in the brain stem. (A) CYP2B1 protein assayed by immunoblotting, showing a significant increase at all three doses of nicotine (3.6-, 2.8-, and 5.8-fold, respectively). Values are means ± SEM of four rats, each assayed three or more times. (B) Representative immunoblot; the arrow shows the position of the immunoreactive CYP2B1 protein band. (C) CYP2B1 mRNA in the brain stem assayed by RT–PCR and Southern blotting showing significant increases at the two highest doses of nicotine tested (2.8- and 7.6-fold, respectively). Values are means ± SEM of four rats assayed three times. (D) Representative Southern blot of CYP2B1 mRNA in the brain stem after treatment with saline and three doses of nicotine for four animals at each dose. Protein and mRNA differences from saline-treated controls: (*) $P < 0.05$, (**) $P < 0.005$, and (***) $P < 0.001$.

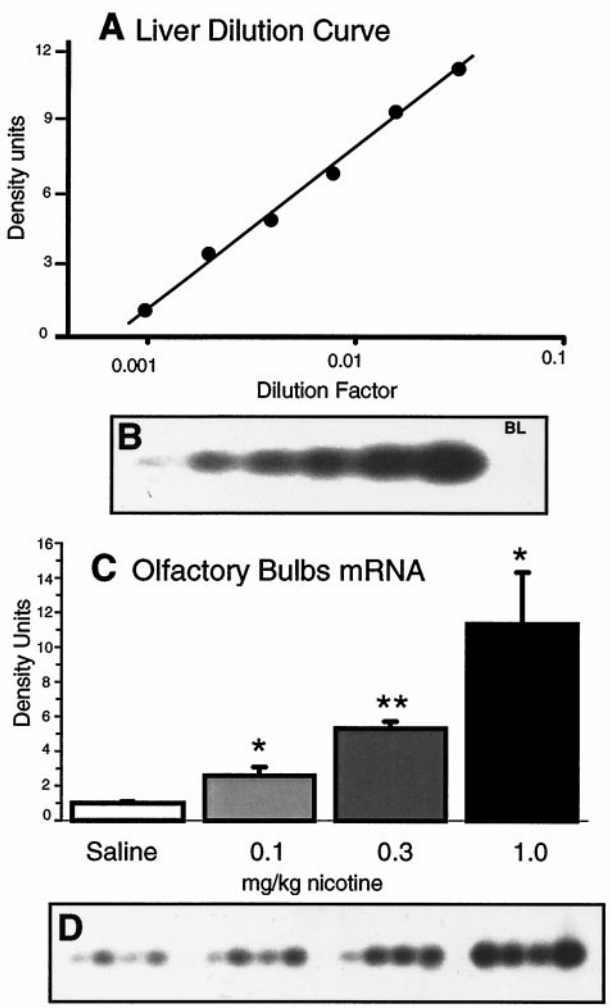

FIG. 3. Southern blotting for CYP2B1 in the brain and liver. (A) Serial dilution of untreated rat liver cDNA template subjected to RT-PCR and Southern blotting for CYP2B1. (B) Representative Southern blot of dilution curve. BL: blank lane, no cDNA. The dilutions ranged from 0.032 to 0.001. The blot is enlarged so that lanes correspond to points on the line graph. (C) Nicotine dose-dependent increase in CYP2B1 mRNA in olfactory bulbs. Values are means ± SEM of four rats; difference from saline-treated controls: (*) $P < 0.05$, and (**) $P < 0.005$. (D) Representative Southern blot of olfactory bulbs from four animals at each nicotine dose. The density of each sample fell within the linear range of the liver dilution curve in A and B.

RT-PCR

CYP2B1 mRNA was detected in liver from untreated rats; liver cDNA was diluted to the range detected in brain, and standard curves were included for every experiment (Fig. 3, A and B). This was to ensure that the range of densities of brain samples on Southern blots was within a log-linear range of detection. CYP2B1 mRNA was detected in all seven brain regions from rats treated with saline and at all three doses of nicotine. The most profound increases in CYP2B1 mRNA were observed in the olfactory bulbs and brain stem (Fig. 3, C and D, and Fig. 2, C and D, respectively). The olfactory bulbs showed significant increases in CYP2B1 mRNA at all three doses of nicotine relative to saline-treated rats, 2.6-fold at 0.1 mg/kg, 5.3-fold at 0.3 mg/kg, and 11.4-fold at 1.0 mg/kg (Fig. 3, B and C). There was also a significant difference in CYP2B1 mRNA between the 0.3 and 1.0 mg/kg doses. The brain stem also showed significant increases in CYP2B1 mRNA at 0.3 mg/kg (2.8-fold,) and 1.0 mg/kg of nicotine (7.6-fold) (Fig. 2, B and C). The 1 mg/kg dose resulted in significantly higher levels of CYP2B1 mRNA than the 0.1 mg/kg and 0.3 mg/kg doses. The frontal cortex and striatum showed increases at the highest nicotine dose of 1.4- and 1.8-fold, respectively; however, these did not reach significance.

CYP2B2 mRNA is present at very low levels in the brain; however, we and Ibach *et al.* [39] have had difficulty detecting either CYP2B2 protein or mRNA and, therefore, we were unable to assess the effect of nicotine treatment on this isozyme.

Immunocytochemistry

There was very little overall immunoreactivity in brain sections from saline-treated animals, consistent with the low levels of immunodetectable CYP2B1 protein (Fig. 1) and mRNA. Most of the staining was seen in the neuropil and axon tracts, probably in glial cells; very little neuronal staining was observed in the saline-treated animals (Table 2). The only areas of intense immunoreactivity were those at the blood–brain barrier, such as the endothelial lining of blood vessels and the choroid plexus. In the olfactory bulbs there was moderate staining of cells in the mitral layer. There was some glial staining in the anterior olfactory nucleus and anterior commissure, and light staining of neurons in the tenia tecta. There was generally low overall neuropilar staining in the cortical regions, with no staining of neurons of the frontal cortex (Fig. 4B), but some light neuronal staining in cingulate cortex area 3 in layers II and III. Thalamic regions showed no staining. The hippocampus stained weakly throughout, with slightly higher levels in the polymorphic layer within the dentate gyrus. The striatum showed very low levels of immunoreactivity compared with surrounding cortical regions. In the cerebellum, the molecular and granular layers showed comparable levels of immunoreactivity. There was moderate staining of small neurons (stellate and basket cells) in the molecular layer, and also staining of glial cells in the subcortical white matter. Purkinje cells showed no immunoreactivity. In the brain stem, which includes the medulla oblongata and the pons, most staining was observed in axonal tracts such as the pyramidal and spinal trigeminal tracts, probably mostly glial. There was some neuronal staining in areas such as the ventral cochlear, trigeminal, and facial nuclei.

After treatment with nicotine two patterns of induction were observed, one where there was increased immunoreactivity in cells, neuropil, and axonal tracts that showed basal staining in saline-treated rats, and a second where cells that showed no CYP2B staining in saline-treated rats became highly immunoreactive. Table 2 shows a summary of the changes in CYP2B staining in cells of the seven regions chosen for immunoblotting after treatment with the highest dose of nicotine, 1.0 mg/kg. In the frontal cortex there was a general overall increase in staining of the neuropil, and a very obvious induction of immunoreactivity in neurons of layers II, III, and IV (Fig. 4). This immunoreactivity increased in a dose-dependent manner similar to that seen on the immunoblots (Table 1). There was also dramatic induction of immunoreactivity in neuronal cells of the piriform cortex (Fig. 5, B and C). In the brain stem, much of the increase in immunoreactivity was seen in the neuropil and axonal tracts, but there was also appearance of neuronal staining in cells that showed no immunoreactivity in control animals (Table 2). In the cerebellum there was no apparent overall change in staining intensity of the molecular and granular cell layers, consistent with results from immunoblots (Table 1). Omission of primary antibody followed by peroxidase quenching eliminated all immuno-

TABLE 2 CYP2B immunocytochemical staining intensity in brain regions and cells of saline- and nicotine (1.0 mg/kg)-treated rats

Brain region	Saline treated	Nicotine treated
Cerebellum (C)		
Granular layer	+ (not glomeruli)	+
Molecular layer	+	+
Purkinje cells	−	−
Frontal cortex (FC)		
Neurons, layers II, III, IV	−	+++
Neuropil	+	++
Hippocampus (HC)		
Dentate gyrus granule cells	−	−
CA 1,2,3 pyramidal cells	−	−
CA 1,2,3 molecular, polymorphic	+	+
Striatum (ST)		
Caudate putamen	±	+
Globus pallidus	−	−
Olfactory tubercle (OT)		
Olfactory tubercle pyramidal layer	−	+++
Islands of Calleja	+	+++
Piriform cortex	−	+++
Tenia tecta	+	+++
Nucleus accumbens shell	+	+
Nucleus accumbens core	−	−
Olfactory bulb (OB)		
Accessory olfactory bulb	+	++
Mitral cells	+	++
Plexiform layers, internal and external	−	+++
Internal granular layer	−	+++
Lateral olfactory tract	−	−
Brain stem (BS)		
Median, dorsal raphe	−	+++
7th Facial nerve	−	−
Medial/superior/lateral vestibular nucleus	±	+++
Pontine reticular nucleus	−	++
Motor trigeminal nucleus	+	+++
Subcoeruleus nucleus	±	++
Substantia nigra reticulata	−	++
Central gray	+	+++
Superior/inferior olivary nucleus	+	+++
Ambiguus nucleus	−	+++
Interpeduncular nucleus	+	+
Facial nucleus	+	++++
Dorsal/ventral cochlear nucleus	+	++
Interposed/lateral cerebellar nucleus	−	+++
Inferior colliculus	−	+

Key: (++++) very strong, (+++) strong, (++) moderate, (+) weak, and (−) no staining.

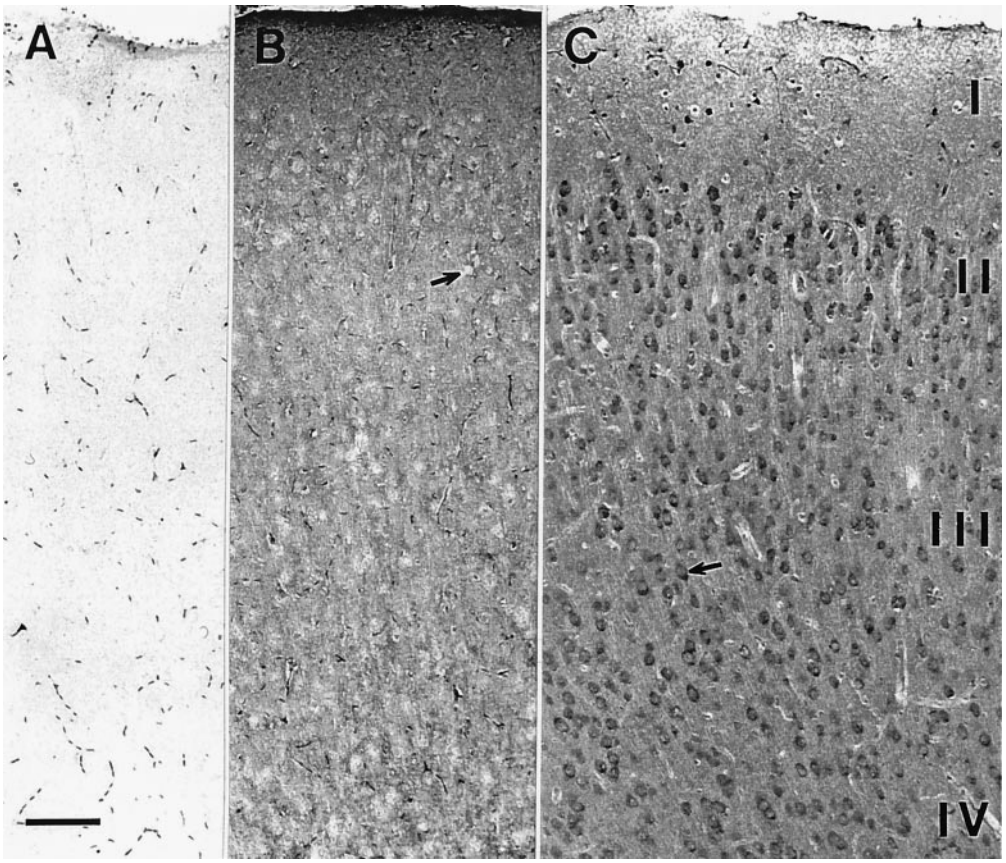

FIG. 4. Immunocytochemical staining for CYP2B of coronal sections of frontal cortex area 3 taken at Bregma 2.7. (A) Control in absence of primary antibody and quenching. (B) Saline-treated animal showing no neuronal staining (arrow) and some neuropilar staining. (C) Nicotine (1.0 mg/kg)-treated animal, showing very strong staining in pyramidal neurons (arrow) in layers II–IV and a moderate increase in overall neuropilar staining. Bar: 100 μm.

reactivity in all regions, and in the absence of peroxidase quenching the only endogenous staining was observed in red blood cells (Figs. 4A and 5A).

DISCUSSION

In this study we have shown that CYP2B1 protein and mRNA are expressed variably across rat brain regions and specific cell types. In addition, we demonstrated that nicotine, a CYP2B1 substrate, can induce CYP2B1 and, hence, its own metabolism. The induction occurred in rat brain, but not in rat liver, and the pattern of induction was brain region- and cell type-specific. The cell-type specific induction occurred both in cells that normally have detectable CYP2B1 and in those that either normally do not express the protein or express CYP2B1 below the detection level. Like many brain CYPs, CYP2B1 was present in very low basal amounts, concentrated primarily in evolutionarily older areas of the allocortex such as the olfactory bulbs, olfactory cortex, hippocampus, cerebellum, and brain stem. Although CYP2B protein was expressed in both glial and neuronal cell populations, expression was cell-specific within regions, as was found previously in rat [40–42] and mouse [6] brains.

Both rodents and humans are known to develop tolerance to the physiological effects of nicotine. This does not occur by altered hepatic metabolism of the drug, but is thought to be mediated, in part, by an increased number and desensitization of nicotinic acetylcholine receptors in certain regions of the brain. However, the changes in receptor density and sensitivity do not account for tolerance completely [22, 23]. One proposed theory is that nicotine metabolites such as cotinine may act as cholinergic antagonists and thus compete for acetylcholine binding sites in the brain [28]. The high degree of localization of CYP2B1 in specific cell types and brain regions after nicotine induction may be sufficient to alter local metabolism of nicotine substantially. For example, in the frontal cortex induction of CYP2B1 (1.8-fold on western blots) is restricted to immunoreactive neurons that occupy approximately 0.6% of the volume of the region used for immunoblotting. This translates to a 300-fold increase in CYP2B1 in these cells, which exceeds untreated hepatic levels (80-fold higher than untreated frontal cortex). This could alter the local concentrations of nicotine and cotinine (the CYP2B1-mediated nicotine metabolite) to which the cholinergic receptors are exposed. Cotinine is present in the brain after exposure to nicotine [18], and it has been

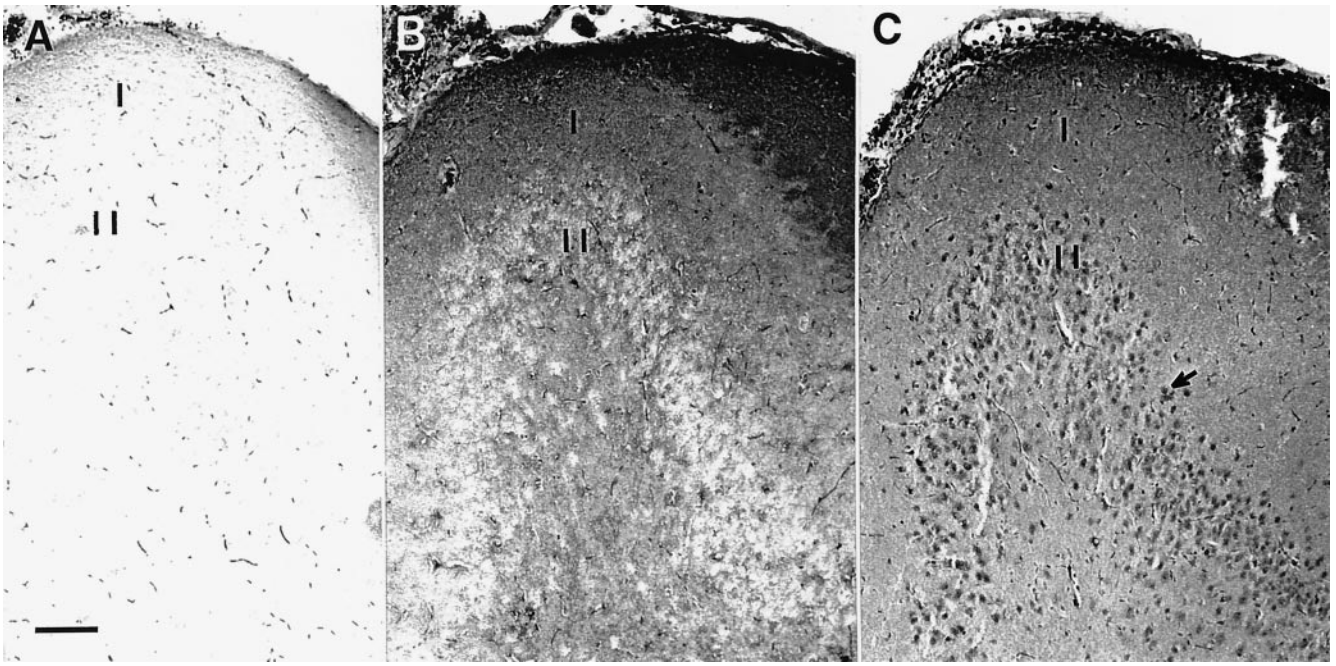

FIG. 5. Immunocytochemical staining for CYP2B of coronal sections of the piriform cortex taken at Bregma 3.2; the left of the figure is dorsal, the right ventral. (A) Control in the absence of primary antibody and quenching. (B) Saline-treated animal showing no neuronal staining. (C) Nicotine (1.0 mg/kg)-treated animal showing intense neuronal staining (arrow) in layer II. Bar: 100 μm.

suggested to play a role in desensitization of nicotinic acetylcholine receptors *in vitro* [19]. Therefore, induction of CYP2B1 in the brain after nicotine exposure (e.g. through smoking) may play a role in the development of central tolerance to nicotine observed both in animal models and in human smokers. After induction by nicotine, CYP2B1 immunoreactivity is seen in regions and cells of the brain that are known to express the α_2 and β_4 nicotinic acetylcholine receptors (e.g. olfactory bulb, olfactory tubercle, piriform cortex, and pyramidal neurons of the frontal cerebral cortex [43]). Interestingly, CYP2B1 protein is induced in some of the same regions and cell types that show up-regulation of nicotinic receptors in response to nicotine, such as frontal cortex pyramidal cells, but not in other regions such as the hippocampus [20, 44].

Although we observed profound induction of CYP2B1 in the brain (greater than 5-fold in some brain regions), we observed no induction of the hepatic form of this enzyme by nicotine. This lack of hepatic induction is consistent with the absence of increase in overall nicotine metabolism in nicotine-treated animals [45] and in human smokers [46]. Tissue-specific regulation of CYPs, and CYP2B in particular, has been reported previously. Acetone treatment decreased CYP2B protein in rat nasal mucosa [47], but induced CYP2B1 in both liver and kidney by increasing the rate of gene transcription [48]. Phenobarbital and acetone treatment increased CYP2B and CYP2E1 activities in rat liver, but had no effect on these CYP activities in rat lung [49]. A possible explanation for the tissue-specific induction of CYP2B1 that we observed is that with the s.c. route of administration of nicotine, the brain experienced much higher blood concentrations of nicotine than the liver, resulting in increased transcription of CYP2B1 in the brain, but not in the liver. However, the level of cell-specificity of CYP2B1 induction in the brain implies that other regulatory processes are also important, for example cell-specific transcription factors.

CYP2B6 is the human homologue of rat CYP2B1, with overlapping substrate specificity [50]. We have detected CYP2B6 in the human brain using an anti-CYP2B1 monoclonal antibody (Miksys S and Tyndale RF, unpublished observations). CYP2B protein has also been detected by others in the human brain, using antibodies to phenobarbital-inducible rat brain protein and to rat CYP2B1/2 [41, 51, 52]; however, its distribution has not been characterized carefully. Although CYP2A6 is the major hepatic enzyme responsible for nicotine metabolism in humans [12], it has not been identified in the human brain. Although human CYP2B6 also metabolizes nicotine [53], this enzyme is expressed predominantly extrahepatically. The larger amounts of liver CYP2A6 result in this being the principal enzyme responsible for human hepatic nicotine metabolism. In the central nervous system, especially following induction by exposure to nicotine, human CYP2B6 may play a quantitatively larger role in central nicotine metabolism, at least in some brain regions.

It is of interest to determine if our observations in the rat extend to the human, with a similar dose-, region-, and cell-specific induction of nicotine-metabolizing CYP2B6 in the brains of cigarette smokers. In addition to inactivating nicotine, CYP2B1 and CYP2B6 can activate many exogenous compounds to toxic and carcinogenic metabolites

[54]. Two such substrates of the CYP2B family are the tobacco-specific nitrosamines NDMA [55] and NNK [56], one of the most precarcinogenic components of tobacco. NNK has been implicated directly in esophageal, lung, and pancreatic cancers [57]; there is also evidence of linkage between exposure to tobacco smoke and brain tumors [58–60]. These data together suggest that CYP2B6 in the human brain could contribute to the development of brain tumors, particularly in smokers, where levels may be higher.

Regulation of expression of the hepatic *CYP2B2* gene is well studied, and induction of hepatic CYP2B1 by phenobarbital occurs principally by increased gene transcription [61]. However, very little is known about the regulation of CYP2B1 in the brain, particularly by inducers that do not increase hepatic CYP2B1. Anandatheervarada *et al.* [24] found increased CYP2B-mediated enzymatic activity in all brain regions examined in response to nicotine treatment, and Schilter and Omiecinski [10] found variable patterns of induction of CYP2B1 mRNA among brain regions in response to phenobarbital. In cultured C6 glioma cells, phenobarbital induction of CYP2B1/2 protein was also found to be under transcriptional regulation [62]. Our data showed similar profiles of increase in CYP2B1 protein and mRNA, e.g. the olfactory bulbs and the brain stem showed the highest increases in both CYP2B1 protein (4.3- and 5.8-fold) and CYP2B1 mRNA (11.4- and 7.6-fold) (Figs. 3 and 2, respectively), indicating that the nicotine regulation likely was mediated through increased transcription or stabilization of mRNA. These data suggest that like the hepatic forms, brain CYP2B1 is regulated at the level of the gene transcript.

In summary, we have shown that nicotine exposure increased the amount of the nicotine-metabolizing enzyme CYP2B1 in rat brain in a region- and cell-specific manner, without altering the hepatic levels of this enzyme. The highly localized nature of induced CYP2B1 in the brain may result in regionally discrete increases in the levels of carcinogenic metabolites of CYP2B substrates such as NNK, thus rendering these cells more susceptible to mutagenesis, genotoxicity, and death. Similarly, nicotine exposure may cause local alterations in the brain of levels of nicotine and its metabolites, such as cotinine, and this localized metabolism may contribute to central metabolic tolerance to nicotine.

We would like to thank Ms. Yvette Grybowski for her technical assistance. This work was funded by MRC Grant MT14173 and the Centre for Addictions and Mental Health.

References

1. Strobel HW, Geng J, Kawashima H and Wang H, Cytochrome P450-dependent biotransformation of drugs and other xenobiotic substrates in neural tissue. *Drug Metab Rev* **29**: 1079–1105, 1997.
2. Hansson T, Tindberg N, Ingelman-Sundberg M and Kohler C, Regional distribution of ethanol-inducible cytochrome P450 IIEI in the rat central nervous system. *Neuroscience* **34**: 451–463, 1990.
3. McFadyen MC, Melvin WT and Murray GI, Regional distribution of individual forms of cytochrome P450 mRNA in normal adult human brain. *Biochem Pharmacol* **55**: 825–830, 1998.
4. Morse DC, Stein AP, Thomas PE and Lowndes HE, Distribution and induction of cytochrome P450 1A1 and 1A2 in rat brain. *Toxicol Appl Pharmacol* **152**: 232–239, 1998.
5. Norris PJ, Hardwick JP and Emson PC, Regional distribution of cytochrome P450 2D1 in the rat central nervous system. *J Comp Neurol* **366**: 244–258, 1996.
6. Volk B, Hettmannsperger U, Papp TH, Amelizad Z, Oesch F and Knoth R, Mapping of phenytoin-inducible cytochrome P450 immunoreactivity in the mouse central nervous system. *Neuroscience* **42**: 215–235, 1991.
7. Lewis DFV and Lake BG, Molecular modeling of mammalian CYP2B isoforms and their interaction with substrates, inhibitors and redox partners. *Xenobiotica* **27:** 443–478, 1997.
8. Warner M and Gustafsson J-A, Cytochrome P450 in the brain: Neuroendocrine functions. *Front Neuroendocrinol* **16**: 224–236, 1995.
9. Hodgson AV, White TB, White J and Strobel HW, Expression analysis of the mixed function oxidase system in rat brain by the polymerase chain reaction. *Mol Cell Biochem* **120**: 171–179, 1993.
10. Schilter B and Omiecinski CJ, Regional distribution and expression modulation of cytochrome P-450 and epoxide hydrolase mRNAs in the rat brain. *Mol Pharmacol* **44**: 990–996, 1993.
11. Volk B, Meyer RP, von Lintig F, Ibach B and Knoth R, Localization and characterization of cytochrome P450 in the brain. *In vivo* and *in vitro* investigations on phenytoin- and phenobarbital-inducible isoforms. *Toxicol Lett* **82/83**: 655–662, 1995.
12. Messina ES, Tyndale RF and Sellers EM, A major role for CYP2A6 in nicotine C-oxidation by human liver microsomes. *J Pharmacol Exp Ther* **282**: 1608–1614, 1997.
13. Nakajima M, Yamamoto T, Nunoya K-I, Yokoi T, Nagashima K, Inoue K, Funae Y, Shimada N, Kamataki T and Kuroiwa Y, Role of human cytochrome P4502A6 in C-oxidation of nicotine. *Drug Metab Dispos* **24**: 1212–1217, 1996.
14. Hammond DK, Bjercke RJ, Langone JJ and Strobel HW, Metabolism of nicotine by rat liver cytochromes P-450. Assessment utilizing monoclonal antibodies to nicotine and cotinine. *Drug Metab Dispos* **19**: 804–808, 1991.
15. Nakayama H, Okuda H, Nakashima T, Imaoka S and Funai Y, Nicotine metabolism by rat hepatic cytochrome P450s. *Biochem Pharmacol* **45**: 2554–2556, 1993.
16. Kyerematen GA, Owens GF, Chattopadhyay B, deBethizy JD and Vesell ES, Sexual dimorphism of nicotine metabolism and distribution in the rat. Studies *in vivo* and *in vitro*. *Drug Metab Dispos* **16**: 823–828, 1988.
17. Jacob P III, Ulgen M and Gorrod JW, Metabolism of (-)-(*S*)-nicotine by guinea pig and rat brain: Identification of cotinine. *Eur J Drug Metab Pharmacokinet* **22**: 391–394, 1997.
18. Crooks PA, Li M and Dwoskin LP, Metabolites of nicotine in rat brain after peripheral nicotine administration. *Drug Metab Dispos* **25**: 47–54, 1997.
19. Dwoskin LP, Teng L, Buxton ST and Crooks PA, (*S*)-(-)-Cotinine, the major brain metabolite of nicotine, stimulates nicotinic receptors to evoke [^{3}H]dopamine release from rat striatal slices in a calcium-dependent manner. *J Pharmacol Exp Ther* **288**: 905–911, 1999.
20. Marks MJ, Stitzel JA and Collins AC, Time course study of the effects of chronic nicotine infusion on drug response and brain receptors. *J Pharmacol Exp Ther* **235**: 619–628, 1985.

21. Benwell ME, Balfour DJ and Anderson JM, Evidence that tobacco smoking increases the density of (-)-[^{3}H]nicotine binding sites in human brain. *J Neurochem* **50**: 1243–1247, 1988.
22. Court JA, Lloyd S, Thomas N, Piggott MA, Marshall EF, Morris CM, Lamb H, Perry RH, Johnson M and Perry EK, Dopamine and nicotinic receptor binding and the levels of dopamine and homovanillic acid in human brain related to tobacco use. *Neuroscience* **87**: 63–78, 1998.
23. Wonnacott S, Characterization of nicotinic receptor sites in brain. In: *Nicotine Psychopharmacology: Molecular, Cellular and Behavioural Aspects* (Eds. Wonnacott S, Russell MAH and Stollerman IP), pp. 227–277. Oxford University Press, Oxford, 1990.
24. Anandatheerthavarada HK, Williams JF and Wecker L, The chronic administration of nicotine induces cytochrome P450 in rat brain. *J Neurochem* **60**: 1941–1944, 1993.
25. Cohen C, Welzl H and Battig K, Effects of nicotine, caffeine, and their combination on locomotor activity in rats. *Pharmacol Biochem Behav* **40**: 121–123, 1991.
26. Corrigall WA and Coen KM, Nicotine maintains robust self-administration in rats on a limited-access schedule. *Psychopharmacology (Berl)* **99**: 473–478, 1989.
27. Nordberg A, Romanelli L, Sundwall A, Bianchi C and Beani L, Effect of acute and subchronic nicotine treatment on cortical acetylcholine release and on nicotinic receptors in rats and guinea-pigs. *Br J Pharmacol* **98**: 71–78, 1989.
28. Schwartz RD and Kellar KJ, Nicotinic cholinergic receptor binding sites in the brain: Regulation *in vivo*. *Science* **220**: 214–216, 1983.
29. Ravishankar H and Padmanaban G, Turnover of messenger RNA, apoprotein and haem of cytochrome P-450b+e. *Biochem J* **229**: 73–79, 1985.
30. Paxinos G and Watson C, *The Rat Brain in Stereotaxic Coordinates*, 2nd Edn. Academic Press, San Diego, CA, 1986.
31. Ghersi-Egea J-F, Perrin R, Leninger-Muller B, Grassiot M-C, Jeandel C, Floquet J, Cuny G, Siest G and Minn A, Subcellular localization of cytochrome P450 and activities of several enzymes responsible for drug metabolism in the human brain. *Biochem Pharmacol* **45**: 647–658, 1993.
32. Bradford MM, A rapid and sensitive method for the quantification of microgram quantities of protein utilizing the principle of protein-dye binding. *Anal Biochem* **72**: 248–254, 1976.
33. Goldfarb I, Korzekwa K, Krausz KW, Gonzalez F and Gelboin HV, Cross-reactivity of thirteen monoclonal antibodies with ten vaccinia cDNA expressed rat, mouse and human cytochrome P450s. *Biochem Pharmacol* **46**: 787–790, 1993.
34. Desrochers M, Christou M, Jefcoate C, Belzil A and Anderson A, New proteins in the rat CYP2B subfamily: Presence in liver microsomes of the constitutive CYP2B3 protein and the phenobarbital-inducible protein product of alternatively spliced CYP2B2 mRNA. *Biochem Pharmacol* **52**: 1311–1319, 1996.
35. Xie W and Rothblum LI, Rapid, small-scale RNA isolation from tissue culture cells. *Biotechniques* **11**: 325–327, 1991.
36. Omiecinski CJ, Hassett C and Costa P, Developmental expression and *in situ* localization of the phenobarbital-inducible rat hepatic mRNAs for cytochromes CYP2B1, CYP2B2, CYP2C6 and CYP3A1. *Mol Pharmacol* **38**: 462–470, 1990.
37. Tyndale RF, Hales TG, Olsen RW and Tobin AJ, Distinctive patterns of $GABA_A$ receptor subunits mRNAs in 13 cell lines. *J Neurosci* **14**: 5417–5428, 1994.
38. Hedlund E, Gustafsson JA and Warner M, Cytochrome P450 in the brain: 2B or not 2B. *Trends Pharmacol Sci* **19**: 82–85, 1998.
39. Ibach B, Appel K, Gebick-Haerter P, Meyer RP, Friedberg T, Knoth R and Volk B, Effect of phenytoin on cytochrome P450 2B mRNA expression in primary rat astrocyte cultures. *J Neurosci Res* **54**: 402–411, 1998.
40. Perrin R, Minn A, Ghersi-Egea J-F, Grassiot M-C and Siest G, Distribution of cytochrome P450 activities towards alkoxyresorufin derivatives in rat brain regions, subcellular fractions and isolated cerebral microvessels. *Biochem Pharmacol* **40**: 2145–2151, 1990.
41. Ravindranath V, Bhamre S, Bhagwat SV, Anandatheerthavarada HK, Shankar SK and Tirumalai PS, Xenobiotic metabolism in brain. *Toxicol Lett* **82/83**: 633–638, 1995.
42. Tirumalai PS, Bhamre S, Upadhya SC, Boyd MR and Ravindranath V, Expression of multiple forms of cytochrome P450 and associated mono-oxygenase activities in rat brain regions. *Biochem Pharmacol* **56**: 371–375, 1998.
43. Happe HK, Peters JL, Bergman DA and Murrin LC, Localization of nicotinic cholinergic receptors in rat brain: Autoradiographic studies with [^{3}H]cytisine. *Neuroscience* **62**: 929–944, 1994.
44. Zhang X, Gong Z-H and Nordberg A, Effects of chronic treatment with (+)- and (−)-nicotine on nicotinic acetylcholine receptors and *N*-methyl-D-aspartate receptors in rat brain. *Brain Res* **644**: 32–39, 1994.
45. Marks MJ, Burch JB and Collins AC, Effects of chronic nicotine infusion on tolerance development and nicotine receptors. *J Pharmacol Exp Ther* **226**: 817–825, 1983.
46. Benowitz NL and Jacob P III, Nicotine and cotinine elimination pharmacokinetics in smokers and nonsmokers. *Clin Pharmacol Ther* **53**: 316–323, 1993.
47. Longo V and Ingelman-Sundberg M, Acetone-dependent regulation of cytochromes P4502E1 and P4502B1 in rat nasal mucosa. *Biochem Pharmacol* **46**: 1945–1951, 1993.
48. Johansson I, Ekstrom G, Scholte B, Purycki D, Jornvall H and Ingelman-Sundberg M, Ethanol-, fasting-, and acetone-inducible cytochromes P450 in rat liver: Regulation and characteristics of enzymes belonging to the IIB and IIE gene subfamilies. *Biochemistry* **27**: 1925–1934, 1988.
49. Lee C, Watt K, Chang A-M, Plopper C, Buckpitt A and Pinderton K, Site-selective differences in cytochrome P450 isoform activities. Comparison of expression in rat and rhesus monkey lung and induction in rats. *Drug Metab Dispos* **26**: 396–400, 1998.
50. Ekins S, VandenBranden M, Ring BJ and Wrighton SA, Examination of purported probes of human CYP2B6. *Pharmacogenetics* **7**: 165–179, 1997.
51. Bhagwat SV, Leelavathi BC, Shankar SK, Boyd MR and Ravindranath V, Cytochrome P450 and associated monooxygenase activities in the rat and human spinal cord: Induction, immunological characterization and immunocytochemical localization. *Neuroscience* **68**: 593–601, 1995.
52. Bhamre S, Anandatheerathavarada HK, Shankar SK, Boyd MR and Ravindranath V, Purification of multiple forms of cytochrome P450 from a human brain and reconstitution of catalytic activities. *Arch Biochem Biophys* **301**: 251–255, 1993.
53. Flammang AM, Gelboin HV, Aoyama T, Gonzalez FJ and McCoy GD, Nicotine metabolism by cDNA-expressed human cytochrome P-450s. *Biochem Arch* **8**: 1–8, 1992.
54. Code EL, Crespi CL, Penman BW, Gonzalez FJ, Chang TKH and Waxman DJ, Human cytochrome P4502B6: Interindividual hepatic expression, substrate specificity, and role in procarcinogen activation. *Drug Metab Dispos* **25**: 985–993, 1997.
55. Stiborova M, Hansikova H and Frei E, Cytochromes P450 2B1 and P450 2B2 demethylate *N*-nitrosodimethylamine and *N*-nitrosomethylaniline *in vitro*. *Gen Physiol Biophys* **15**: 211–223, 1996.

56. Guo Z, Smith TJ, Ishizaki H and Yang CS, Metabolism of 4-(methylnitrosamino)-1-(3-pyridyl)-1-butanone (NNK) by cytochrome P450IIB1 in a reconstituted system. *Carcinogenesis* **12**: 2277–2282, 1991.
57. Hecht SS, Biochemistry, biology, and carcinogenicity of tobacco-specific *N*-nitrosamines. *Chem Res Toxicol* **11**: 559–603, 1998.
58. Koppang N, Rivenson A, Dahle HK and Hoffmann D, A study of tobacco carcinogenesis, LIII: Carcinogenicity of *N′*-nitrosonornicotine (NNN) and 4-(methylnitroamino)-1-(3-pyridyl)-1-butanone (NNK) in mink (*Mustala vison*). *Cancer Lett* **111**: 167–171, 1997.
59. Lee M, Wrensch M and Miike R, Dietary and tobacco risk factors for adult onset glioma in the San Francisco Bay area. *Cancer Causes Control* **8**: 13–24, 1997.
60. Tredaniel J, Boffetta P, Saracci R and Hirsch A, Environmental tobacco smoke and the risk of cancer in adults. *Eur J Cancer* **29A**: 2058–2068, 1993.
61. Kemper B, Regulation of cytochrome P450 gene transcription by phenobarbital. *Prog Nucleic Acid Res Mol Biol* **61**: 23–64, 1998.
62. Geng J and Strobel HW, Expression, induction and regulation of the cytochrome P450 monooxygenase system in the rat glioma C6 cell line. *Brain Res* **784**: 276–283, 1998.